交通部中央氣象局委託研究計畫成果報告

植被、地表對台灣降水及天氣之研究（一）

計畫類別：□國內　　■國外

計畫編號：MOTC-CWB-93-3M-03

執行期間：93 年 2 月 1 日至 93 年 12 月 31 日

計畫主持人：　商文義

執行單位： Sun Reasearch

中華民國 93 年 12 月 18 日

九十三年度政府部門科技計畫期末摘要報告

計畫名稱：植被、地表對台灣降水及天氣之應用研究

審議編號：		部會署原計畫編號：	MOTC-CWB-93-3M-03
主管機關：	交通部中央氣象局	執行單位：	Purdue University
計畫主持人：	商文義	聯絡人：	
電話號碼：	0021-765-494-7681	傳真號碼：	0021-765-496-1210
期程：	93 年 1 月 1 日至 93 年 12 月 31 日		
經費：（全程）	仟元	經費(年度)	650 仟元

執行情形：

1. 執行進度：

	預定（%）	實際（%）	比較（%）
當年全程	100	100	0

2. 經費支用：

	預定	實際	支用率（%）
當年全程	650 仟元	650 仟元	100

3. 主要執行成果：探討一維植被, 土壤濕地理論模式的建立

4. 計畫變更說明：無

5. 落後原因：無

6. 主管機關之因應對策（檢討與建議）：

中央氣象局委託計畫『植被、地表對台灣降水及天氣之應用研究』
期末報告
by

Wen-Yih Sun
Department of Earth and Atmospheric Sciences
Purdue University
December 18, 2004

A complete atmosphere-surface system may include the following components:

(a) Atmospheric model, (b) snow-vegetation-soil model to handle the land-surface, and (c) snow-water model to handle the water body beneath the atmosphere. We have developed the Purdue Regional Climate Model, which has been applied to simulate weather and climate under various conditions.

We have also developed the one-dimensional vegetation-soil model to handle interaction between snow-vegetation-soil and atmosphere. In order to study the water-body for pond, marsh, as well as the sea and ocean, we are working on a one-dimensional snow-sea-ice model. The model consists of snow, sea-ice, and sea water, which is much more complicated than the pond-model used in the tropical and sub-tropical regions, it also takes a much longer effort to develop it. On the other hand, the application of the model discussed here is wider than the pond or marsh model, as proposed in our original proposal. It is noted that snow-sea-ice model can directly be applied to the pond when its basin is assumed saturated without infiltration, which has been applied in the existing pond models. However, it will be better to couple the snow-sea-ice model and the soil-vegetation-snow model, as well as to simplify the snow-sea-ice model when it is applied to simulate the rice-field and marsh. Hence, that will be the focus of the second year project.

The main focuses of 2004-project are

1. develop a comprehensive one-dimensional model for water body;
2. collect the observational data in order to verify the model;
3. calculate the detailed heat and moisture budgets at water surface; and
4. incorporate the snow-vegetation-soil model to Purdue Regional Climate Model to simulate the 1998 flood in China and Korea

The more detail description of the one-dimensional snow-sea-ice model

1. Introduction of the one-dimensional snow-sea-ice model

In the Polar Regions the energy budgets of atmosphere and ocean are strongly affected by the presence of snow/sea ice. As a result of high albedo, snow and sea ice dramatically reduce the amount of shortwave radiative energy available at the surface. Because of its low thermal conductivity, snow/sea ice also significantly restricts heat exchange between the ocean and the atmosphere. The variation of sea ice distribution, concentration, and thickness has been widely recognized as one of the strongest signals in climate changes (Houghton et. al 1990). In the past, several sea-ice models and observational studies (Semtner 1976, Washington et al. 1976, Mellor 1986, Mellor et al. 1986, Price et al. 1986, Maykut and Perovich 1987, Josberger 1987, Morison et al. 1987, Omstedt 1990, McPhee 1992, Jin et al. 1994, Kiehl et al. 1996, McPhee et al. 1999, and others) have been presented to study the thermodynamics and dynamics of sea ice and interactions among the atmosphere, sea ice and sea water. Most numerical models were applied to simulate the seasonal or annual variation of sea ice instead of the daily evolution due to the limitation of observational data.

Recently, SHEBA provided daily observations, including upward and downward radiative fluxes, precipitation, wind, humidity, air and snow temperatures, sensible heat flux, as well as temperature, salinity, and density of sea water in 1997-1998. SHEBA, sponsored by the National Science Foundation and the Office of Naval Research, is a large, interdisciplinary study that is motivated by climate change issues. SHEBA has two goals: (1) understanding the ice-albedo and cloud-radiation feedbacks; and (2) using this understanding to improve models. The schematic diagram of snow and ice sites on SHEBA floe is shown in Fig. 1. SHEBA also provided data of snow and sea ice depths. Here, we present a one-dimensional snow/sea ice-ocean model and comparisons between the model simulations and observations during November 1997 and January 1998, when the observed temperature, salinity, and density of sea water are available at JOSS Data Management Center CODIAC, a data management system, which offers scientists access to research and operational geophysical data. We have also performed sensitivity test of the effect of snow depth and ventilation (Waddington et al. 1996). Results show that snow thickness is a crucial factor in determining the depth of sea ice. Consequently, it strongly

influences the temperature and heat transfer. Simulations also reveal that ventilation is significant in this study.

The multi-layer snow/sea ice-ocean model is based on conservation of energy, mass, and momentum (Chern and Sun 1998). The mixed-layer ocean model is used to predict the water temperature, salinity, density, and turbulent kinetic energy, while the snow/sea ice model is used to predict the thickness, temperature, and heat flux of snow/sea ice. The transfers at the interfaces between the atmosphere and snow/sea ice, water and sea ice, and the open ocean and the atmosphere are also included. Mathematical formulation and physical processes of the mixed-layer ocean model are presented in Section 2. We then briefly outline the formulas of the one-dimensional snow/sea ice model in Section 3. A simple parameterization for snow ventilation is presented in Section 4. The comparisons between the modeled simulations and observations are discussed in Section 5, which is followed by Summary.

2. One-Dimensional Mixed-Layer Ocean Model

The models are applied to simulate the interactions among the atmosphere, snow, sea ice, and sea water. It is noted that the current velocity is excluded due to the lack of observational data and the horizontal pressure gradient. It is also noted that shortwave radiation is not calculated due to the high latitude of SHEBA floe in the winter. The equations for a one-dimensional ocean model are

$$\frac{\partial(T\Delta z)}{\partial t} = H/(c_w\rho_w) - \delta(\overline{w'T'}) + \gamma(T_{obs} - T)\Delta z \tag{2.1}$$

$$\frac{\partial(S\Delta z)}{\partial t} = -\delta(\overline{w'S'}) + \gamma(S_{obs} - S)\Delta z \tag{2.2}$$

$$\rho_w = \rho_0(1.0 - \alpha_\rho T_c + \beta_\rho S) \tag{2.3}$$

where T is water temperature, c_w is the specific heat capacity of sea water, Δz is the layer-thickness, S is salinity, ρ_w is the density of seawater, H is the heating, $\overline{w'T'}$ and $\overline{w'S'}$ are heat and salinity fluxes, respectively. $\delta(\phi)$ is defined as

$$\delta(\phi)_k = \phi_{k-top} - \phi_{k-bottom} \tag{2.4}$$

Here subscripts *k-top* and *k-bottom* stand for the value at the top and bottom of the k-layer. Because the advection is not included, we may include the Newtonian forcing with γ=

1/(6 hr) in temperature and salinity equations so that they will not significantly depart from observations. The time scale of 6 hr is chosen such that it is much longer than the time scale of convection in the upper mixed layer but short enough for adjusting to the change of mean profile due to advection. The simulations without γ will also be discussed.

The density of water ρ_0=1000 Kg m^{-3}, and coefficients of α_p and β_p are as follows:

$$\alpha_\rho = (77.5 + 8.75T_c) \times 10^{-6} \tag{2.5}$$

$$\beta_\rho = (779.1 - 1.66T_c) \times 10^{-3} \tag{2.6}$$

where Tc= T-273.15 K, according to Kraus and Businger (1994).

The heating is given by

$$H = \{H_{f-m} - H_{sfc}\} \tag{2.7}$$

where, H_{f-m} is the net latent heat released from freeze or melt, and H_{sfc} is the net surface heating.

H_{sfc} in (2.7) is

$$H_{sfc} = \begin{cases} Hs + HL - Hp + RL^{\uparrow} - RL^{\downarrow}, & \text{at open water surface} \\ 0, & \text{otherwise} \end{cases} \tag{2.8}$$

$\overline{w'T'}$ at the open water surface is included in Hs of (2.8). It is also assumed $\overline{w'S'}$ =0 at the water surface. The downward and upward longwave radiations at the surface are

$$R\lambda^{\downarrow} = \varepsilon_{sw} R\lambda^{\downarrow}_{air} \tag{2.9}$$

and

$$RL^{\uparrow} = \varepsilon_{sw} \sigma T_{sfc}^4 \tag{2.10}$$

where $R\lambda^{\downarrow}_{air}$ is downward longwave radiance reaching the sea surface, emittance ε_{sw} is 0.98, and Stefan-Boltzmann constant σ is 5.67x10^{-8} W m^{-2} K^{-4}.

Hs, HL, and Hp are the surface sensible heat flux, latent heat flux, and heat transfer associated with precipitation at the surface, respectively (Lynch-Stieglitz 1994, hereafter L-S). They follow the similarity equations:

$$Hs = c_a \rho_a \overline{w_a' \theta_a'} = -c_a \rho_a u_* \theta_* = \rho_a c_a c_h |V_a| (\theta_{sfc} - \theta_a) \tag{2.11}$$

$$HL = L_v \rho_a \overline{w_a' q_a'} = -L_v \rho_a u_* q_* = L_v E_{evap} = L_v \rho_a c_h |V_a| (q_{sfc} - q_a) \tag{2.12}$$

where $|V_a|$ is the wind speed near the surface, and

$$Hp = \begin{cases} c_w \rho_w T_a \mathrm{Pr}, & \text{for } \mathrm{T_a} \geq 273.15\ K \\ c_{sn} \rho_{new-snow} T_a Ps, & \text{for } \mathrm{T_a} < 273.15\ K \end{cases} \quad (2.13)$$

in which Pr and Ps are precipitation rate for rain and snow (in m s^{-1}), c_w and c_{sn} are specific heat capacity of water and snow, respectively. T_a is the air temperature, q_{sfc} is 0.98 of the saturated mixing ratio at ocean surface, and $\rho_{new-snow}$ = 170 Kg m^{-3} is the density of the new fallen snow.

From (2.3), we obtain the buoyancy

$$\frac{-g\rho'}{\rho_0} = g\alpha_\rho T - g\beta_\rho S \quad (2.14)$$

The eddy fluxes $\overline{w'T'}$ and $\overline{w'S'}$ are derived from

$$\overline{\mathrm{w'T'}} = -\kappa_\mathrm{T}\left(\frac{\partial \mathrm{T}}{\partial \mathrm{z}}\right) \quad (2.15)$$

and

$$\overline{\mathrm{w'S'}} = -\kappa_\mathrm{T}\left(\frac{\partial \mathrm{S}}{\partial \mathrm{z}}\right) \quad (2.16)$$

The eddy coefficient κ_T (m^2 s^{-1}) is a function of turbulent kinetic energy according to Sun (1989, 1993a, b).

The mass of the top-layer water will change due to evaporation, precipitation, melt or freeze:

$$\frac{\partial(\rho_w \Delta z)}{\partial t} = \{\rho_w \mathrm{Pr} + \rho_{new-snow} Ps - E_{evap}\}_{surface} - M_{f-m} \quad (2.17)$$

in which $\{\rho_w \mathrm{Pr} + \rho_{new-snow} Ps - E_{evap}\}_{surface}$ is applied at the open water surface only. M_{f-m} $=(H_{f-m}/L_f)$ is the mass loss (gain) due to freeze (melt) at the open water surface or the ice-water interface. Since the ocean model is coupled with the snow/sea ice model, whenever the sea water is frozen, it was automatically taken as sea ice and resulting in the decrease of the top-layer water. On the other hand, melt of sea ice increases the mass of water beneath sea ice according to (2.17).

The freezing point of the seawater $T_{sw(fre)}$ is a function of salinity:

$T_{sw(fre)} = 273.15 - 55S$ (S in Kg/Kg) (Maykut 1985) (2.18)

Similarity equations are applied at the atmospheric surface layer to calculate u_*, θ_*, and q_*.

The heat flux between sea ice and water was proposed by Josberger (1987) and McPhee (1992):

$$\overline{w'T'} = c_{hsw} u_{*sw} (T_{ml} - T_{sw(fre)}) \tag{2.19}$$

where c_{hsw}=0.006, u_{*sw}=0.5 cm s^{-1} is friction velocity under sea ice, T_{ml} is the mixed layer temperature. u_{*sw} varies from 0 to 2 cm s^{-1} and $T_{ml} - T_{sw(fre)}$ varies from 0 to 0.32 K according to the 1984 Marginal Ice Zone Experiment (MIZEX 84) and the 1988 Coordinate Eastern Arctic Experiment (CEAREX 88)(McPhee 1992, Kiehl et al. 1996). u_{*sw} is 0.88 cm s^{-1} in the Weddell Sea during the Antarctic Zone Flux Experiment (ANZFLUX) (McPhee et al. 1999). When the surface water becomes freezing or coexists with sea ice, the conservation of enthalpy, which will be defined in Section 3, is applied to calculate the change of phase.

3. Basic Equation for One-dimensional Snow/Sea Ice Model

The mass, thickness, and density of a snow layer are defined as

$$M_{sn} = M_s + M_w, \tag{3.1a}$$

$$\Delta z_{sn} = \Delta z_s + \Delta z_w, \tag{3.1b}$$

$$\rho_{sn} = \left(\rho_s \Delta z_s + \rho_w \Delta z_w\right) / \Delta z_{sn} \tag{3.1c}$$

where subscripts "sn", "s", "w" are related to entire snow (=dry snow + liquid water), dry snow, and liquid water, respectively. The temperature (T_{sn}) can be calculated from equation of enthalpy within snow

$$\left[\frac{\partial (H_{en} \Delta z_{sn})}{\partial t}\right]_k = (F^{sn}_{k+1/2} - F^{sn}_{k-1/2}), \tag{3.2}$$

where enthalpy is:

$$H_{en} = \{(C_w \Delta z_w + C_s \Delta z_s)(T_{sn} - 273.15) + \rho_w \Delta z_w L_{ei}\} / \Delta z_{sn} \tag{3.3}$$

The heat fluxes at the top and bottom of layer k (except at the surface) is defined as

$$F^{sn}_{k\pm1/2} = \left[-K_{sn}(\frac{\partial T_{sn}}{\partial z}) - Rs^{\downarrow}_{sn} - H_{flow} - \phi c_a \rho_a \delta(\overline{w'T'}) - [c_{sn} \rho_{sn} T_{sn} w_{blow}]_{sfc}\right]_{k\pm1/2}, \tag{3.4}$$

where $C_{sw} \approx C_w = 4.218 \times 10^6$ J $(m^3 K)^{-1}$ according to Verseghy (1991) and L-S. The heat capacity of solid phase of snow/ice C_i is

$$C_i = 1.9\times10^6 \frac{\rho_i}{\rho_{ice}},\ [\mathrm{J\,(m^3\ K)^{-1}}] \tag{3.5}$$

where $\rho_{ice} = 920\ \mathrm{Kg\ m^{-3}}$.

The diffusivity in (3.3) can be written as

$$K_i = 0.021 + 2.5\times(\rho_i/10^3)^2\ \mathrm{W\,m^{-1}K^{-1}}\ \text{(Brandt and Warren 1993)} \tag{3.6a}$$

$$K_w = 0.6\ \mathrm{W\,m^{-1}\,K^{-1}} \tag{3.6b}$$

and

$$K_{sn} = (K_i \Delta z_i + K_w \Delta z_{sw})/\Delta z_{sn} \tag{3.6c}$$

The heat flux at the snow surface is

$$F_{1/2} = H_{sfc} = Hs + H\lambda - Hp + R\lambda^{\uparrow} - R\lambda^{\downarrow} \tag{3.7}$$

where longwave and shortwave radiations are

$$RL^{\downarrow} = \varepsilon_{sn} RL^{\downarrow}_{air} \tag{3.8a}$$

$$RL^{\uparrow} = \varepsilon_{sn}\sigma T_{sn}^4 \tag{3.8b}$$

and

$$Rs^{\downarrow} = (1 - r_{sn}) Rs^{\downarrow}_{air} \tag{3.8c}$$

The snow emissivity $\varepsilon_{sn} = 0.98$. Albedo of snow/ice is a function of wavelength and cloudiness (Greenfell and Perovich 1984) and varies from 0.2 to 0.9. Following Anderson (1976) and Liston and Hall (1995), we assume

$$r_{sn} = \begin{cases} 1.0 - 0.247[0.16 + 110(\rho_{sn}/1000)^4]^{1/2} & \text{for } \rho_{sn} < 450\ \mathrm{kg\ m^{-3}} \\ 0.6 - \rho_{sn}/4600 & \text{for } \rho_{sn} \geq 450\ \mathrm{kg\ m^{-3}} \\ 0.25 & \text{for } \rho_{sn} > 920\ \mathrm{kg\ m^{-3}}\ (\mathrm{ice + water}) \end{cases} \tag{3.9}$$

The decrease of shortwave radiance within the k^{th} layer of snow/ice is calculated as

$$\{Rs^{\downarrow}\}_{k-bottom} = \{Rs^{\downarrow}\}_{k-top} \exp\{-\alpha_{sn}\Delta z_{sn}\}_k \tag{3.10}$$

Subscripts *k-bottom* and *k-top* indicate at the bottom and top of the k^{th} layer, respectively. The attenuation α_{sn} of solar energy is a function of depth, property of snow/ice, cloudiness, solar zenith angle, etc. (Greenfell and Maykut 1977; Warren 1982; Jin et al. 1994; Ebert et al., 1995.). For simplicity, α_{sn} is assigned a representative value of 20 $\mathrm{m^{-1}}$ for snow and 7 $\mathrm{m^{-1}}$ for ice (Verseghy 1991; Gu and Stefan 1990).

We finally get the change of mass within each layer

$$\frac{\partial(\rho_{sn}\Delta z)}{\partial t} = M_{f-m} + \{\rho_w \Pr + \rho_{new-snow} Ps - E_{evap} - \rho_{sn} w_{blow}\}_{sfc} + \{net\ water\ flow\} \quad (3.11)$$

M_{f-m} is the change of phase caused by freezing-melting, the second term is applied at snow/ice surface, and $\{net\ water\ flow\}$ is the net water accumulation from water flowing through that layer.

Following Kojima (1967), Pitman et al. (1991), and L-S, the snow compactness between time interval Δt ($= t^{n+1} - t^n$) due to vertical stress and viscosity is parameterized:

$$\rho_i^{(n+1)} = \rho_i^n + \{.5 \times 10^{-7} \rho_i^n g N_k \times \exp[\, 14.643 - \frac{4000}{\min(T, 273.16)} - 0.02\rho_i^n \,]\}\Delta t \quad (3.12)$$

where gN_k is the weight of the snow pack above the midpoint of layer k.

Snow and ice start melting, when the temperature is above 0 °C. A portion or entire water trapped inside snow/sea-ice can freeze, if it is below 0 °C. At the sea ice-water interface, seawater freezes and leaves salinity behind, when the temperature is below freezing point according to Eq (2.23).

4. Observation and simulation of sea water density, salinity, and temperature

The data at Data Management Center CODIAC-WWW include the vertical profiles of water temperature, salinity and density between 287.14 and 393.23 on SHEBA Days (January 1, 1997 is Day 1). The towers provided air temperature, dew point, wind direction and speed, pressure, long- and shortwave radiations, precipitation, and sensible heat flux started from SHEBA Day 304. The coupled snow/sea ice and ocean models were integrated from October 31 (SHEBA Day 304) to January 27, 1998 (SHEBA Day 392) for 89 days continuously, with the observed air temperature, wind, precipitation (or the observed snow depth), and downward longwave radiation at 2 m height as the external forcing from the atmosphere. The measured sea water temperature and salinity on Day 304 were used as the initial condition for the oceanic mixed-layer model to calculate the sea water temperature, salinity, density, and turbulent kinetic energy. But we did not calculate current velocity due to the lack of the pressure gradient force and the initial current data. The snow and sea ice measured at Baltimore and Seattle sites will be used as the initial conditions to simulate the evolution of snow/sea ice and interactions between atmosphere and snow/sea ice in the Arctic region.

The radiative cooling at the surface increases the thickness of sea-ice during the winter time. Meanwhile, the snow/sea ice surface temperature also decreases with time. It creates a well mixed layer just beneath the sea ice, because the temperature at the interface is around -2C, which is cooler than the water temperature in the lower layer.

The sea water density, salinity, and temperature observed at Day 303.0 (indicated by A), 330.5 (indicated by B), 365.7 (indicated by C), and 392.0 (indicated by D) are shown in Fig. 1. The simulated values without γ (no Newtonian forcing in (2.1) and (2.2) are shown in Fig. 2, in which we can see that a mixed layer developed in the upper ocean mainly due to salinity distribution. The general pattern of the simulations is consistent with observations, show in Fig. 1. However, the results also indicate the important of the advection terms, which are not included in (2.1) and (2.2). In order to simulate the effect of advection terms, we set γ=1/6hr and show the results in Fig. 3, which is much closer than those in Fig. 2 compared with observations in Fig.1.

6. Summary

A one-dimensional snow/sea ice-ocean model with its application to the Arctic Ocean is presented. The model includes a mixed-layer ocean model, a multi-layer snow/ice model, and interfaces between atmosphere and snow/sea ice, sea ice and water, as well as atmosphere and open ocean.

Numerical simulations of the SHEBA experiment between November 1997 and January 1998 show that net longwave radiation deficit caused cooling of snow/sea ice and freezing of the sea water beneath the sea ice. The latent heat released from freezing at ice-water interface was transferred upward through snow/sea ice with a strong temperature gradient. The atmosphere and sea water also provided a small amount of sensible heat fluxes to snow/sea ice. We used the observed snow thickness to determine the effective precipitation rate. Therefore, the snow depth remained consistent with the measurement. The results also indicate that the horizontal advection and drifting of sea ice should be included in the ocean model to reproduce the observed property of sea water and current velocity, even though the snow and sea ice were not sensitive to the detailed

profiles of salinity and water temperature. Finally, more observations and advanced models are needed to simulate the drifting snow and ventilation in the Arctic realistically.

Acknowledgments: SHEBA has been sponsored by the National Science Foundation and the Office of Naval Research. Computing resources provided by NCAR and NPACI at San Diego Supercomputer Center are also appreciated.

Captions:

Fig. 1. (a) Sea water density, (b), salinity, and (c) temperature observed at Day 303.0 (indicated by A), 330.5 (indicated by B), 365.7 (indicated by C), and 392.0 (indicated by D).

Fig. 2. Same as Fig. 1, except for model simulations without Newtonian forcing

Fig. 3. Same as Fig. 1, except for model simulations with Newtonian forcing γ=1/6hr.

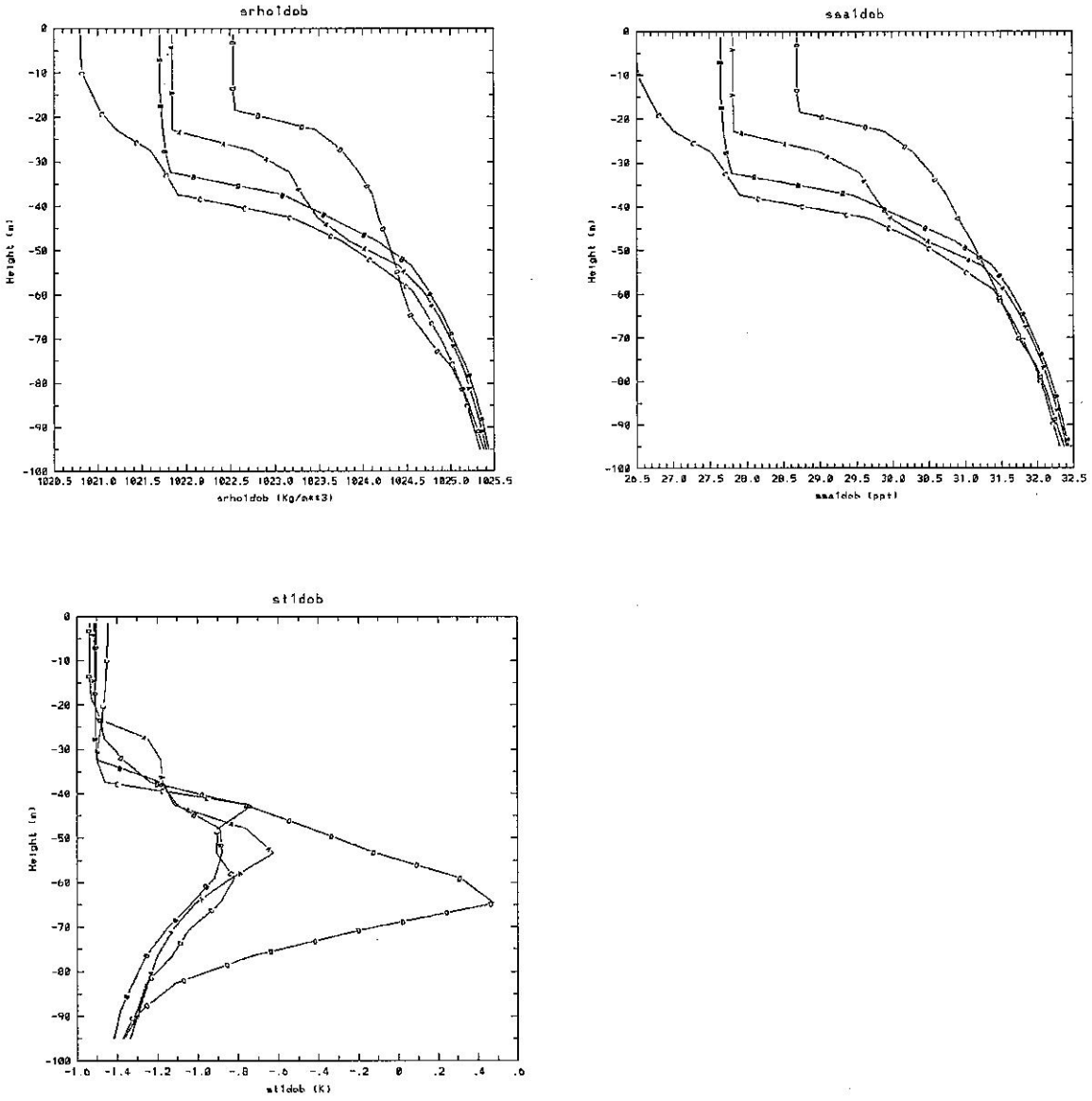

Fig. 1: (a) Sea water density, (b), salinity, and (c) temperature observed at Day 303.0 (indicated by A), 330.5 (indicated by B), 365.7 (indicated by C), and 392.0 (indicated by D).

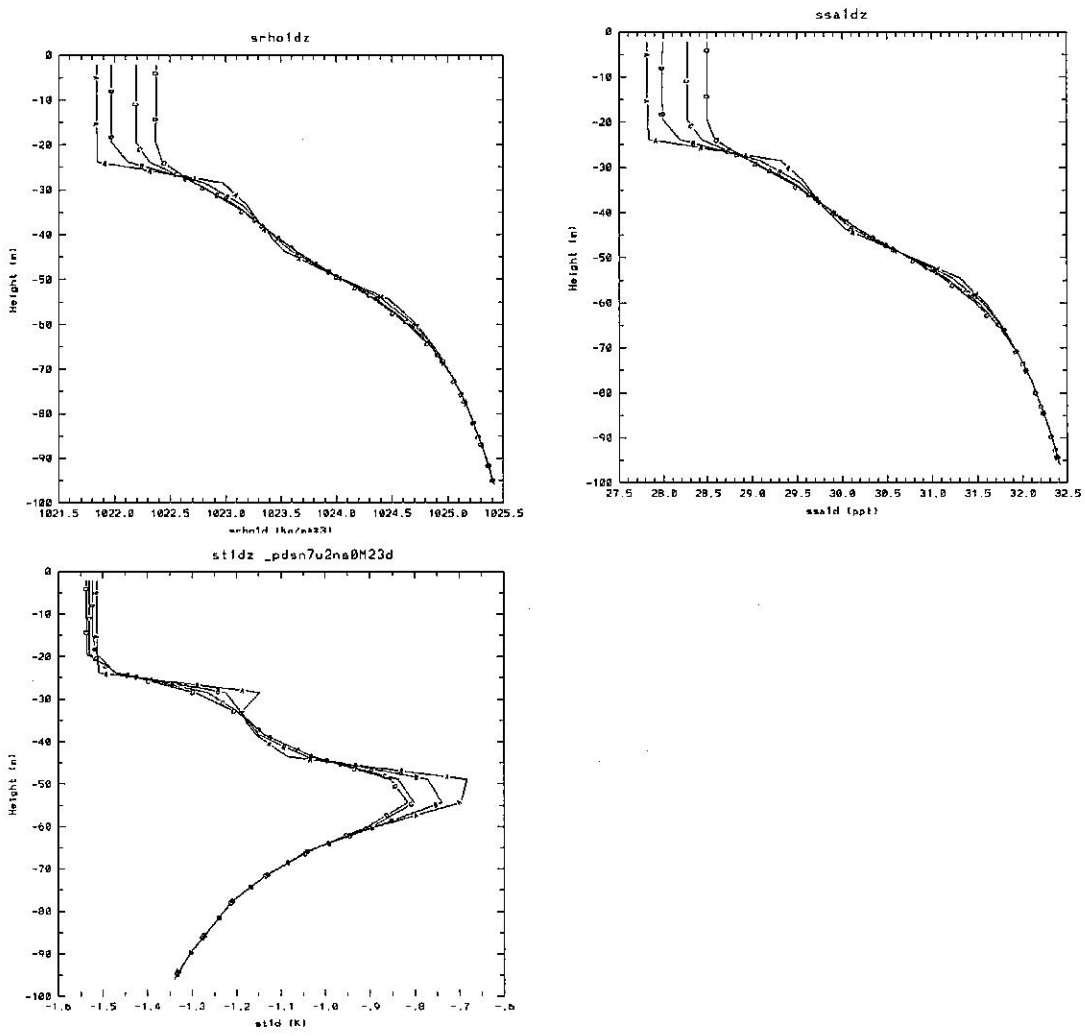

Fig. 2. Same as Fig. 1, except for model simulations without Newtonian forcing

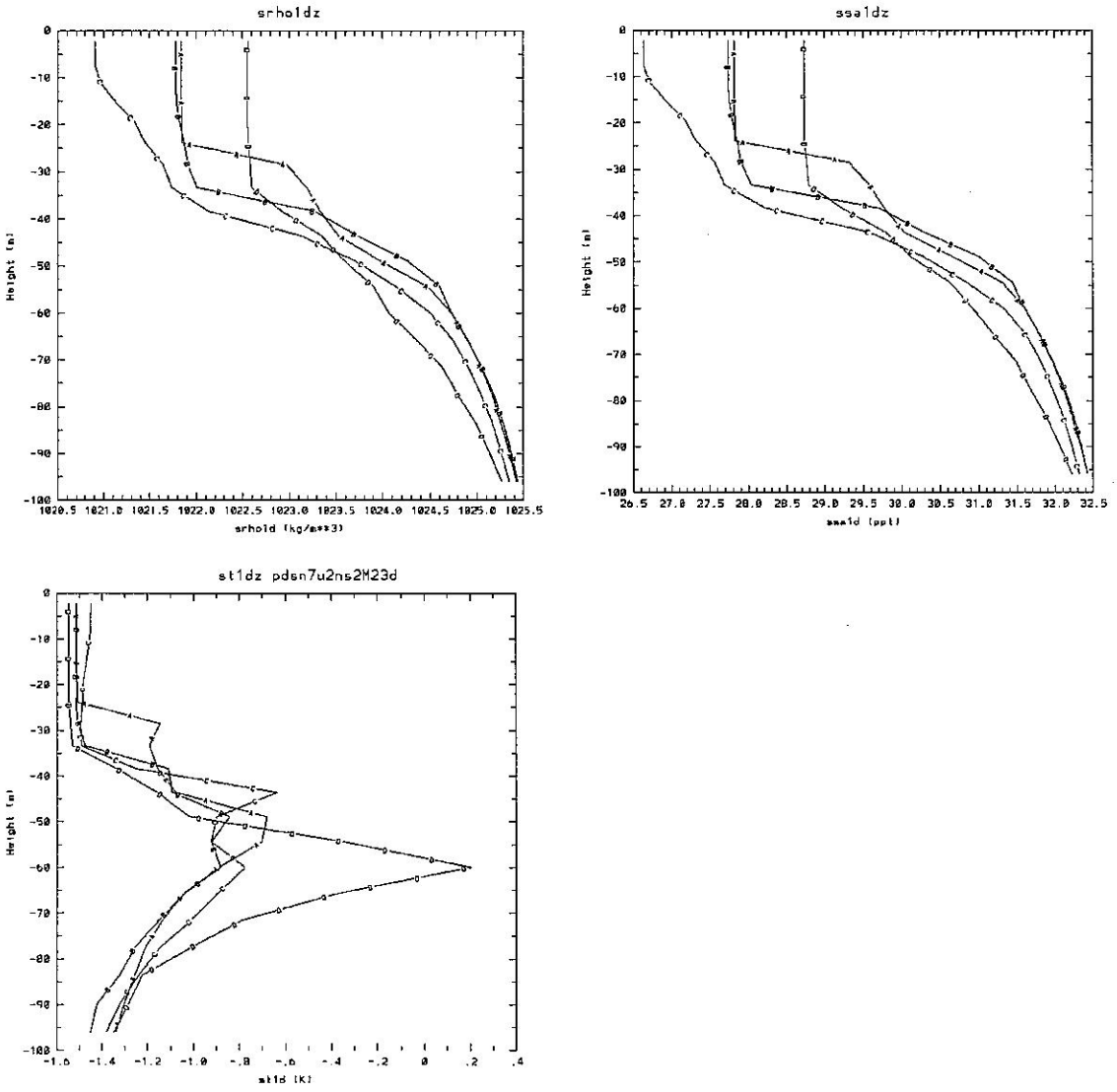

Fig. 3. Same as Fig. 1, except for model simulations with Newtonian forcing γ=1/6hr.

References:

Albert, M. R., 1996: Modeling heat, mass, and species transport in polar firn. Annals of Glaciology 23, 138-143.

Brandt, R., and S. G. Warren, 1993: Solar-heating rates and temperature profiles in Antarctic snow and ice. J. Glaciology, 39, 99-109.

Chern, J.D., 1994: Numerical simulation of cyclogenesis over the western United States. Ph.D. thesis, Department of Earth and Atmospheric Sciences, Purdue University, W. Laf. IN. 178 pp.

Chern, J. D., and W. Y. Sun, 1998: Formulation and validation of a snow model. A11A-06, 1998 Fall Meeting, AGU, Supplement to EOS, AGU, 79,45. F96. Nov. 10, 1998.

Colbeck, S. C., 1989: Air movement in snow due to wind pumping. J. of Geophyw. Res., 35, 120, 209-213.

Cunningham, J., and Waddington, E. D., 1993: Air flow and dry depsoition of no-sea salt sulfate in polar firn: paleoclimate implications. Atmospheric Environment 27A (17/18): 2943-2956.

Gjessing , Y. T., 1977: The filtering effect of snow. In: Isotopes and impurities in ice and snow. IAHS Publication No. 118: 199-203.

Houghton, J. T., G. J. Jenkins and J. J. Ephraums, eds., 1990: Climate change: the IPCC scientific assessment. Cambridge, Cambridge University Press.

Jin, Z., K. Stamnes, W. F. Weeks, and S-C. Tsay, 1994: The effect of sea ice on the solar energy budget in the atmosphere-sea ice-ocean system: A model study. J. Geophys. Res. 99, 25,281-25,294.

Jordan, R., 1991: A one-dimensional temperature model for a snow cover. U. S. Army Crops of Engineers, Cold Regions Research and Engineering Laboratory, Special Report 91-16, 49 pp.

Josberger, E. G., 1987: Bottom ablation and heat transfer coefficients from the 19893 Marginal Ice Zone Experiments. J. Geophys. Res. 92, 7012-7016.

Kiehl, J. T., J. J. Hack, G. B. Bonan, B. Boville, B. P. Briegleb, D. L. Williamson, P. J. Rasch., 1996: Description of the NCAR Community Climate Model (CCM3). NCAR/TN-420+STR. NCAR Technical Note, Boulder, CO.

Kojima, K., 1967: Densification of seasonal snow cover. Physics of Ice and Snow, Proc. Int. Conf. on Low Temperature Sciences, Sapporo, Japan, Institute of Low Temperature Science, Hokkaido University, 929-952.

Kraus, E. B., and J. A. Businger, 1994: Atmosphere-Ocean Interaction (2nd Ed.), Oxford University press. 362 pp.

Lynch-Stieglitz, M., 1994: The development and validation of a simple snow model for the GISS GCM. J. Climate, 7, 1842-1855.

Maykut, G. A., 1985: An introduction to ice in polar ocean. Applied Physics Lab./U. of Washington Publ. (APL-UW 8510).

Maykut, G. A., and D. K. Perovich, 1987: The role of shortwave radiation in the summer decay of a sea ice cover. J. Geophys. Res., 92, 7032-7044.

McPhee, M. G., 1992: Turbulence heat flux in the upper ocean under sea ice. J. Geophys. Res., 97, 5365-5379.

McPhee, M. G., C. Kottmeier, and J. H. Morison, 1999: Ocean heat flux in the central Weddell Sea during Winter. J. Phys. Oceanogr. 29, 1166-1179.

Mellor, G. L., M. G. McPhee, and M. Steele, 1986: Ice-sea water turbulent boundary layer interaction with melting and freezing. J. Phys. Oceanogr. 16, 1829-1846.

Mellor, M., 1986: Mechanical behavior of sea ice, in The Geophysics of Sea Ice, NATO ASI Ser., Ser. B146, edited by N. Untersteiner, pp. 165-281, Plenum, New York, 1986.

Morison, J. H., M. G. McPhee, and G. A. Maykut, 1987: Boundary layer, upper ocean, and ice observations in Greenland sea marginal ice zone. J. Geophys. Res., 92, 6987-7011.

Moritz, R. E., and Perovich (eds), 1996: Surface Heat Budget of the Arctic Ocean Science Plan , ARCSS/OAII Report Number 5. University of Washington, Seattle, 64 pp.

Omstedt, A., 1990: A coupled one-dimensional sea ice-ocean model applied to a semi-enclosed basin. Tellus, 42A, 568-582.

Pitman, A. J., Z-L. yang, J. G. Cogley, and A. Henderson-Sellers, 1991: Description of bare essentials of surface transfer for the Bureau of Meteorological Research Centre AGCM, BRMC, Australia, BMRC Research Report No. 32, 117pp.

Price, J. F., R. A. Weller, and R. Pinkel, 1986: Diurnal cycling: observations and models of the upper ocean response to diurnal heating, cooling and wind mixing. J. Geophys. Res. (Ocean) 91, 8411.

Semtner, A. J., Jr., 1976: A model for the thermodynamic growth of sea ice in numerical investigations of climate. J. Phys. Oceanogr., 6, 378-389.

Sun, W. Y. , 1989: Diffusion modeling in a convective boundary layer. *Atmospheric Environment . 23*, 1205-1217.

Sun, W. Y., 1993a: Numerical simulation of a planetary boundary layer: Part I. Cloud-free case. *Beitrage zur Physik der Atmosphare. 66*, 3-16..

Sun, W. Y., 1993b: Numerical simulation of a planetary boundary layer: Part II. Cloudy case. *Beitrage zur Physik der Atmosphare. 66,* 17-30.

Verseghy, D. L., 1991: CLASS- A Canadian land surface scheme for GCMS, I: Soil model. Int. J. Climatol., 11,111-133.

Waddington, E. D., J. Cunnungton, J., and S. L. Harder, 1996: The effects of snow ventilation on chemical concentrations. NATO ASI. Series, Vol. 143 (Edited by Wolff and Bales) 403-451.

Washington, W. M., A. J. Semtner, C. Parkinson, and L. Morrison, 1976: On the development of a seasonal change sea-ice model. J. Phys. Oceanogr., 6, 679-685.